Journal of Materials Science and Engineering B 7 (9-10) (2017) 229-236
doi: 10.17265/2161-6221/2017.9-10.004

# Anti-reflection Coating Solar Cell Structure Based on Conductive Nanoparticles

Hana M. Mousa[1], Mohammed M. Shabat[2] and Alhassen K. Ouda[1]

*1. Physics Department, Al Azhar University, Gaza P.O. Box 108, Gaza Strip, Palestine*

*2. Physics Department, Islamic University, Gaza P. O.Box 108, Gaza Strip, Palestine*

**Abstract:** In this paper, we investigate for the first time antireflection coating structure for silicon solar cell where CNPs (conductive nanoparticles) film layer is sandwiched between a semi-infinite glass cover layer and a semi-infinite silicon substrate. The transmission and reflection coefficients are derived by the transfer matrix method and simulated for values of unit cell sizes, gab widths in visible and near-infrared radiation. In addition, the absorption, reflection coefficients are examined for several angles of incidence of the TE (transverse electric) polarized guided waves. Numerical results provide an extremely high absorption, if nanoparticles are suitably located and sized. The absorptivity of the structure achieves 100% at gab width of 3.5 nm and CNP layer thickness of 150 nm.

**Key words:** Solar cells, nanoparticles, antireflection, transfer matrix method, silicon.

## 1. Introduction

Silicon technology is the most widely used one for solar cells, mainly due to a good efficiency-to-cost ratio and great reliability [1]. As the thickness of the absorption layer decreases, the energy-conversion efficiency drops dramatically and this is the main drawback of thin-film solar cells. Moreover, reflection is undesirable and causes insertion losses. It is well known that the application of one or more ARC (antireflection coating) layer on the front surface of silicon cells reduces the amounted reflection of the incident light leading to improve the device performance [2-4]. The theory of antireflection coating is examined by many authors [5, 6]. The matrix method [7, 8] is usually employed for calculation of reflection coefficient. Chen et al. [9] have presented approach of metamaterial antireflection. It reduces the reflection and enhances transmission near a specifical frequency over a wide range of incidence angles for both TE (transverse electric) and TM (transverse magnetic) polarizations. Bouhafs et al. [4] have made a theoretical study of the antireflection coatings on silicon solar cells. In recent decades, there has been a growing progress in the technology of nanoparticles for fabricating solar cell structures due to their high efficiency in light trapping in the proposed structures.

Nanoparticles can be embedded inside the solar cell, near the p-n junction. Some researchers have shown that the scattering of solar radiation from nanoparticles, if suitably located and sized, may considerably improve the functioning of the thin-film cells [10-12]. The light is scattered and trapped into the silicon substrate by multiple and high-angle scattering, causing an increase of the effective optical path length in the cell and, consequently, enabling the improvement of its efficiency. Since the first work exploiting suchan option [13], many papers have investigated thin-film solar cells enhanced by means of scattering from gold [14, 15] and silver [16, 17] nanoparticles. Atwater et al. [18] have embedded metal nanoparticles inside the solar cell. This makes use of the strong local field enhancement around the

**Corresponding author:** Mohammed M. Shabat, Ph.D., professor, Dr., research field: optoelectronics.

metal nanoparticles to increase absorption in the surrounding semiconductor material. This local field generates charge carriers in the semiconductor and becomes particularly useful in materials with small carrier diffusion lengths. Lastly, light can be converted into surface plasma polaritons, which are electromagnetic waves that travel along the interface between a corrugated metal back contact and the semiconductor absorber layer. Polaritons excited at this interface can trap light and guide it laterally into the solar cell. Since solar cell width is much greater than thickness, absorption can be greatly increased especially among long-wavelength photons.

Shabat and Ubeid [19] have studied the antireflection coatings in waveguide structures with silicon nanoparticles interlayer and reported the optimization of the structure for solar cells. Other multilayered waveguide structure [20] containing nanoparticle has numerically been investigated showing the importance of nanoparticles in minimizing the light reflection of such structures. Chung, K. et al. [21] formulated a cubic array of conductive particles as universal effective medium at visible and infrared frequencies and predicted the relative electric permittivity $\varepsilon_r$ and magnetic permeability $\mu_r$ with good accuracy for the entire range of the particle sizes ($b$) and unit cell sizes ($a$). This paper aimed to analyze numerically the possibility of improving the performance of a planar waveguide silicon solar cell under the solar spectrum AM1.5 by incorporating CNPs layer (conductive nanoparticles) between a semi-infinite glass cover layer and a semi-infinite silicon substrate layer. The absorption coefficient of the structure is inferred from the transmission and reflection coefficients that are derived by the transfer matrix method at various angles of incidence and for different values of $\varepsilon_r$ (different gab widths) at constant $\mu_r$ and at constant $\varepsilon_r$ for different values of $\mu_r$ (different unit cell sizes) in visible and near-infrared radiation. The paper also examines the effect of the CNPs layer thickness on the absorption coefficient of the TE polarized.

## 2. Model and Theory

This work predicts anti-reflection coating structure. The film layer is gold CNPs (conductive nanoparticles) sandwiched between a semi-infinite dielectric cover layer and a semi-infinite substrate layer. Light is incident from glass ($n_0$ = 1.47) onto CNPs film. The permittivity $\varepsilon_r$ and permeability, $\mu_r$ of the CNPs film are characterized [19] by

$$\varepsilon_r = \varepsilon_h \frac{b}{a}\left[\frac{b}{g} + \frac{2b}{a} + \frac{g}{a}\left(\frac{g}{b} + \frac{2g}{a}\right)\right],$$

$$\mu_r = \left[1 - \frac{b'^2}{a^2}\right]\left[\frac{b}{a} + \frac{g}{a}\left(1 - \frac{b'^2}{a^2}\right)\right]^{-1} \qquad (1)$$

and $$b'^2 = \left(\frac{\cosh\phi - 0.5}{\cosh\phi - 1}\right)\left(b - 2l_{sD}\tanh\phi\right)^2$$

where $\varepsilon_h$ is the relative permittivity of the host dielectric material, $b$ is the particle size, $a$ is the unit cell size, g is the gap between particles ($a = b + g$), $l_{SD}$ is the skin depth and $\Phi = b/2l_{SD}$. As apparent from the model and Eq. (1), $\varepsilon_r$ can be turned over a very wide range by varying the gab width $g$ and fixing the unit cell size $a$ below the skin depth ($a$ = 20 nm), in this case $\mu_r$ = 1, while $\mu_r$ can be independently tuned by varying $a$ at constant g. The substrate is assumed to be silicon ($n_s$ = 3.77-$i$0.012) (see Fig. 1). A beam of light undergoes reflection at ($i$) and the transmitted portion undergoes another reflection at ($ii$), $E_{r1}$, $E_{t1}$ are the sum of all reflected, transmitted beams at ($i$) respectively. $E_{i2}$, $E_{t2}$ represent the sum of all incidents, transmitted beam at ($ii$) respectively. The optical parameters of the structure are studied using the transfer matrix method which is widely used for reflection and transmission calculations of multilayer structures. The transfer matrix is the matrix which relates to the incident and reflected waves at the input layer with the incident and reflected waves at the output layer [7, 20].

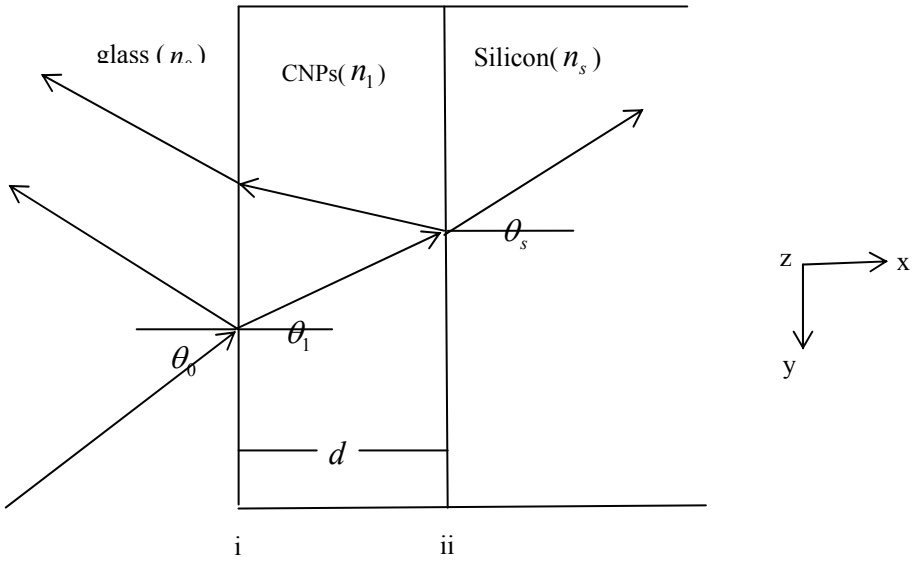


**Fig. 1 Light interfering in a thin film of CNPs between glass cover layer and silicon layer.**

Following the notation and approach in Refs. [1, 4, 19, 20] by using Maxwell's equation and then implementing the continuous boundary conditions of the electric fields $E$ and magnetic fields $B$, where the components of both fields are parallel to the interface to be continuous, we get**:**

$$\begin{aligned} E_0 + E_{r1} &= E_{t1} + E_{i1} \\ E_{i2} + E_{r2} &= E_{t2} \end{aligned} \tag{2}$$

and

$$\begin{aligned} &B_0 \cos(\theta_0) - B_{r1} \cos(\theta_0) = B_{t1} \cos(\theta_1) - B_{i1} \cos(\theta_1) \\ &B_{i2} \cos(\theta_1) - B_{r2} \cos(\theta_1) = B_{t2} \cos(\theta_s) \end{aligned} \tag{3}$$

where the generic equation relating to electric fields and magnetic fields is

$$B = n\sqrt{\varepsilon_0 \mu_0} E \tag{4}$$

The phase difference is

$$\delta = \left( \frac{2\pi}{\lambda_0} \right) n d \cos(\theta_1) \tag{5}$$

with $\lambda_0$ being the incident wavelength and $d$ is the thickness of CNPs layer.

$$E_{i2} = E_{t1} e^{-i\delta}, E_{i1} = E_{r1} e^{-i\delta} \tag{6}$$

By aid of the upper equations, the following matrix system is obtained:

$$\begin{vmatrix} E_0 + E_{r1} \\ y_0 (E_0 - E_{r1}) \end{vmatrix} = \begin{vmatrix} \cos(\delta) & \dfrac{i \sin(\delta)}{y_1} \\ i y_1 \sin(\delta) & \cos(\delta) \end{vmatrix} \begin{vmatrix} E_{t2} \\ y_s E_{t2} \end{vmatrix} \tag{7}$$

where

$$y_0 = n_0 \sqrt{\varepsilon_0 \mu_0} \cos(\theta_0), y_1 = n_1 \sqrt{\varepsilon_0 \mu_0} \cos(\theta_1),$$

$$y_s = n_s \sqrt{\varepsilon_0 \mu_0} \cos(\theta_s)$$

The 2 × 2 matrix in Eq. (6) is called the transfer matrix, which is generally represented by

$$M = \begin{vmatrix} m_{11} & m_{12} \\ m_{21} & m_{22} \end{vmatrix}$$

For a multilayer stack of N thin films, Eq. (6) can then be generalized as:

$$\begin{vmatrix} E_i \\ B_i \end{vmatrix} = M_1 M_2 \ldots\ldots M_N \begin{vmatrix} E_{ii} \\ B_{ii} \end{vmatrix} \tag{8}$$

Dividing the matrix equations by $E_0$ and using the reflection and transmission amplitudes as $r = \frac{E_{r1}}{E_0}$, $t = \frac{E_{t2}}{E_0}$, the reflection coefficient $R = |r|^2$ is [19]:

$$R = \frac{\left[n_0 \cos(\theta_0) - n_s \cos(\theta_s)\right]^2 + \left[\frac{n_0 n_s}{n_1}\frac{\cos(\theta_0)\cos(\theta_s)}{\cos(\theta_1)} - n_1 \cos(\theta_1)\right]^2 \tan^2(\delta)}{\left[n_0 \cos(\theta_0) + n_s \cos(\theta_s)\right]^2 + \left[\frac{n_0 n_s}{n_1}\frac{\cos(\theta_0)\cos(\theta_s)}{\cos(\theta_1)} + n_1 \cos(\theta_1)\right]^2 \tan^2(\delta)} \quad (9)$$

And the transmission coefficient is

$$T = \frac{n_s}{n_0}.\frac{\left[2n_0 \cos(\theta_0)\right]^2}{\left[n_0 \cos(\theta_0) + n_s \cos(\theta_s)\right]^2 + \left[\frac{n_0 n_s}{n_1}\frac{\cos(\theta_0)\cos(\theta_s)}{\cos(\theta_1)} + n_1 \cos(\theta_1)\right]^2 \tan^2(\delta)} \quad (10)$$

The absorption coefficient A (λ) is given by application of the law of conservation of energy

$$A(\lambda) = 1 - R(\lambda) - T(\lambda) \quad (11)$$

Where λ is the operating wavelength of the light and the angle of refraction is related to the incidence angle $\theta_0$ by the Snell's law

$$n_0 \sin\theta_0 = n_1 \sin\theta_1 = n_s \sin\theta_s \quad (12)$$

## 3. Numerical Results and Discussion

The numerical calculations of Eq. (1) in Ref. [19] predict independently the exact values of $\mu_r$ and $\varepsilon_r$. Fig. 2a [21] displays a graph of permeability of conductive particles of gold (CNPs) versus the unit cell size ($a$) at a skin depth of 30 nm while maintaining ($g/a$) constant at 0.1, $\mu_r$ can be tuned between the value of 1 and 0.4. And the $\varepsilon_r$ remains constant value of 20. Fig. 2b illustrates the variation of permittivity of CNPs with the gab width $g$ and fixing the unit cell size below the skin depth ($a$ = 20 nm), in this case $\mu_r$ = 1, $\varepsilon_r$ is independently tuned between values of 42 and 2.

Eqs. (9)-(11) have been solved numerically to find out the reflectance, transmittance and absorption of TE polarization versus the incident wavelength for different incident angles, gab widths, cell sizes, and CNPs layer thicknesses. The results of the simulations are displayed in Figs. 3-6.

Fig. 3 displays the reflected and the absorbed TE polarization versus the incident wavelength for many values of incident angles ($\theta$ = 0°, 50°, 70°). An increase in the reflection coefficient with the increase in angles of incidence can be noticed in the wavelength range (λ = 400-600nm) and (λ = 1,000-1,600nm). Reflectance has minimal values of (0, 0.04, 0.045) while absorption attains maximum values of (1, 0.96, 0.95) about (λ = 800, 900, 1000nm), for ($\theta$ = 70°, 50°, 0°) respectively. It is worth to note that at ($\theta$ = 0°), the absorption coefficient attains maximum of 0.95 and minimum of 0.62 in a wide wavelength range of (400-1,600 nm). The reflection and absorption coefficients versus the operating wavelength at normal incidence for several fixed values of the unit cell size ($a$) of CNPs layer are plotted in Fig. 4. At cell size of values (250, 150, 50 nm), the magnetic permeability of CNPs ($\mu_r$) increases to the values of (0.579, 0.728, 0.953) and its refractive index $n_1$ changes to the values of (3.4, 3.816, 4.367) respectively. As depicted in Fig. 4, at cell size 250 nm, it shows minimum reflectance of 0.192 and maximum absorption of 0.87 at wavelength around 400 and 700 nm. The influence of variation of the gab width $g$ on the reflection and absorption of TE waves is presented in Fig. 5. As it can be seen in the figure, at

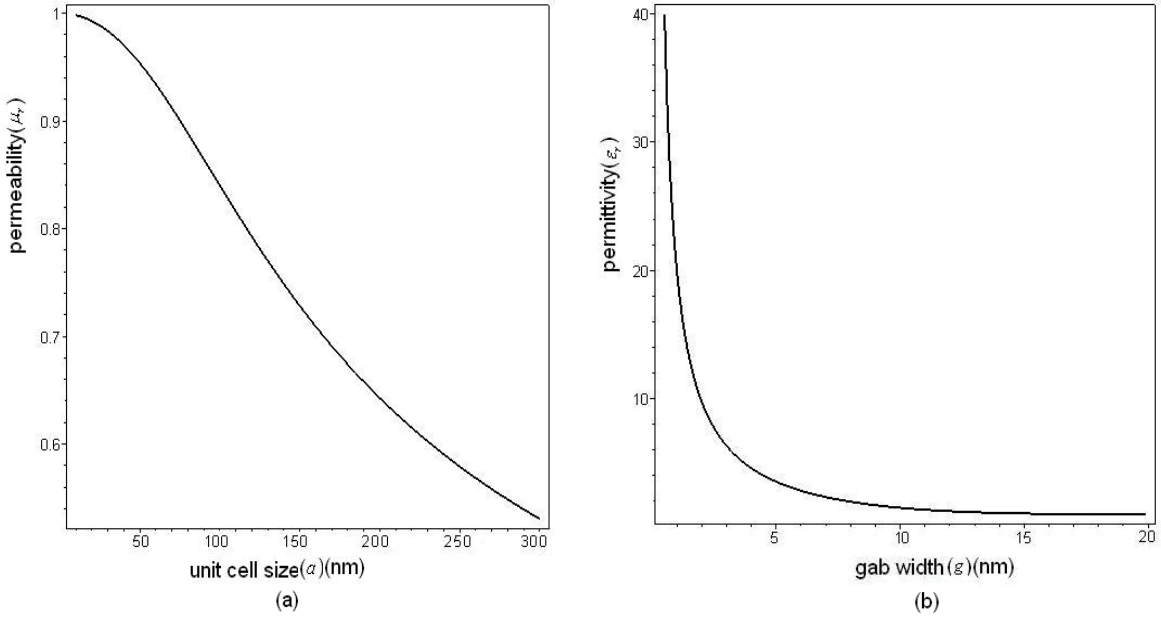


**Fig. 2 (a) Permeability of conductive particles of gold versus the unit cell size, $l_{SD} = 30nm, (g/a) = 0.1$ and (b) Permittivity of conductive particles of gold versus the gab width, *a* = 20 nm [13].**

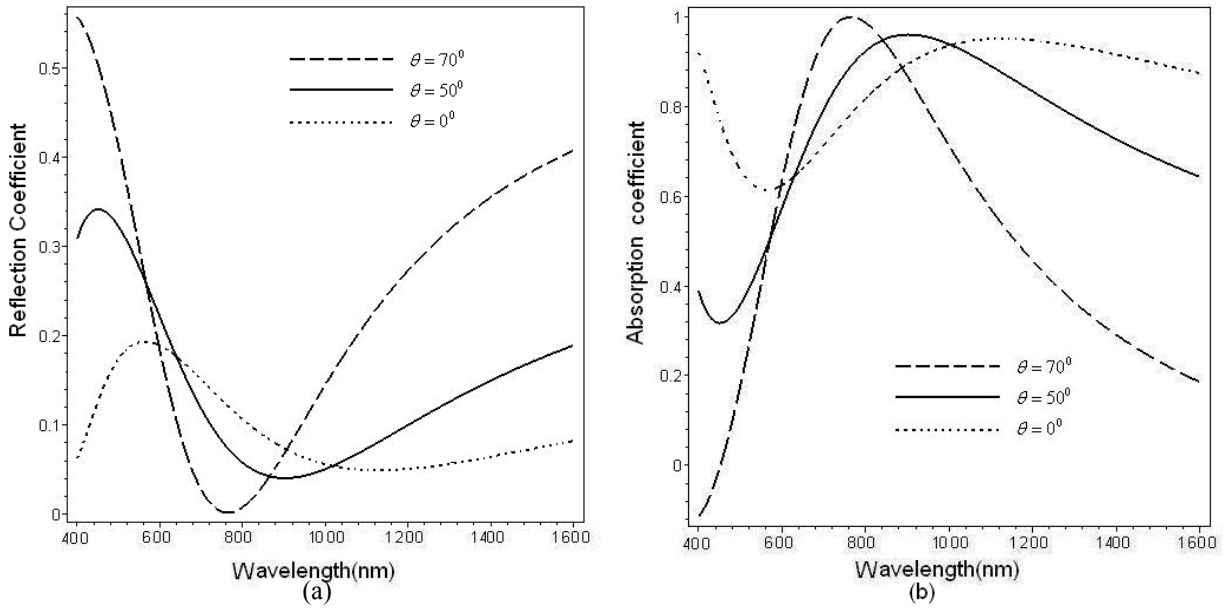


**Fig. 3 (a) Reflection; (b) Absorption of TE polarization versus the wavelength for different incident angles, d = 150 nm, g = 5 nm, $\mu_r = 1$.**

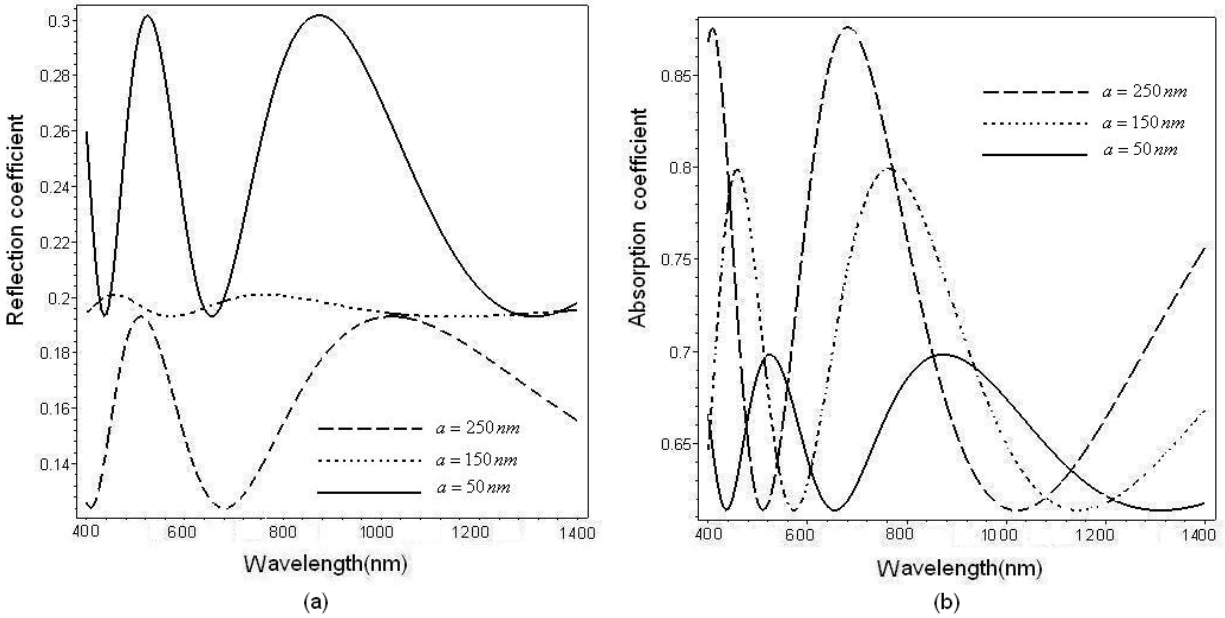


**Fig. 4 (a) Reflection coefficient; (b) Absorption coefficient of TE polarization versus the wavelength for different unit cell sizes (a), $\varepsilon_r = 20$ and d = 150 nm, $\theta = 0°$.**

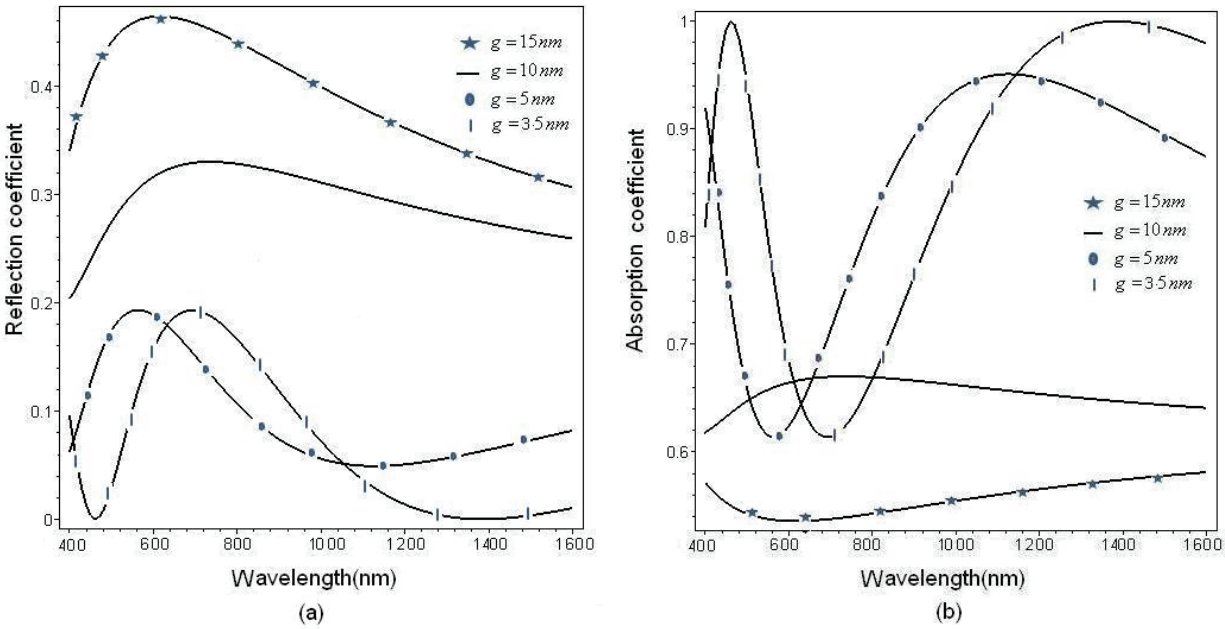


**Fig. 5 (a) Reflectance; (b) Absorption of TE polarization as a function of normal incident wavelength for different gab widths (g), $\mu_r = 1$, d = 150 nm.**

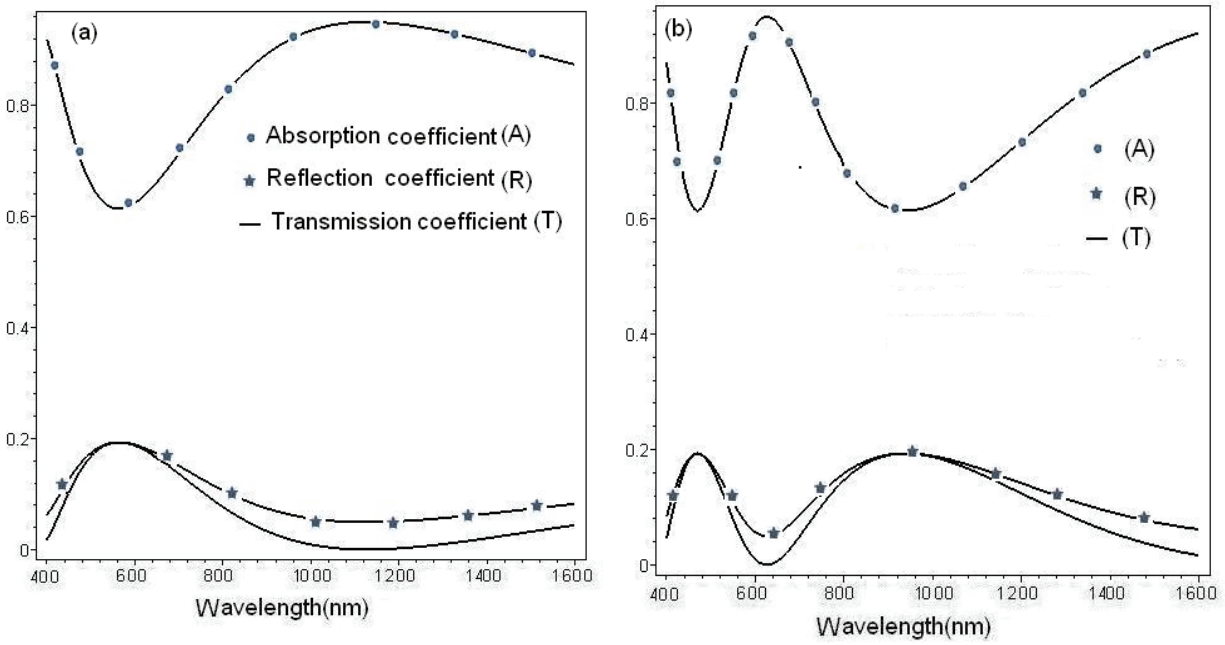


**Fig. 6 Absorption, reflection and transmission coefficient as a function of the normal incident wavelength for (a) d = 150 nm, (b) d = 250 nm, g = 5 nm, $\mu_r = 1$.**

gab width of values (15, 10, 5, 3.5 nm), the electric permittivity of CNPs ($\varepsilon_r$) varies to the values of (1.05, 1.5, 3.53, 5.33) and its refractive index $n_1$ changes very slightly to (1.025, 1.224, 1.879, 2.3) respectively. Reflectance increases by increasing the gab width $g$ (decrease of $n_1$). If $g$ is held constant at 3.5 nm, it achieves reflection coefficient of (0) at wavelength of (450, 1,400 nm) respectively and the absorption coefficient peaks to 1 at wavelength of the same values. For $n_1 = 2.3$, minimum reflectance spectra and high absorption power are achieved since $n_1$ is approximately closed to $\sqrt{n_0 n_s}$ for single layer ARC under normal incidence. This indicates that $g = 3.5$ nm at ARC thickness of 150 nm improves the absorptivity of the considered structure and ARC process. In Fig. 6, the reflection, transmission and absorption coefficients are plotted versus the light wavelength for ARC thickness of values (150, 250 nm). It is interesting to show that the absorption coefficient peaks sharply to 0.95 in the wavelength range of (600-1,400 nm) at thickness of 150 nm whereas it drops off sharply away from the peak to 0.6 at a thickness of 250 nm in the same wavelength range, demonstrating the sensitivity to variations in ARC thickness. As a comparison between the absorption at normal incidence of conventional anti-reflective coating structure where the CNPs are replaced by a silicon nitride ($siN_x$) layer and the absorption of the proposed structure [23, 24] shows that the absorption is nearly zero for the conventional structures which confirm that the implementation of CNPs layer—with suitable nanoparticles size—adjacent to silicon layer dramatically reduces the reflection and greatly enhances the absorption in a wide frequency spectrum at a normal incidence.

## 4. Conclusions

In this communication, a new tri-layered structure consisting of CNPs has been investigated in order to improve the optical absorption of silicon solar cells. Reflection, transmission and absorption are derived, simulated and analyzed. It is demonstrated that the enhanced maximum optical absorption can be achieved by optimizing both the thickness of CNPs layer and nanoparticles size.

## References


[1] Singh, R. 2009. "Why Silicon Is and Will Remain the Dominant Photovoltaic Material." *J. Nanophotonics* 3 (1): 032503.

[2] Dobrowolski, J. A., Poitras, D., Ma, P., Vakil, H., and Acree, M. 2002. "Toward Perfect Antireflection Coatings: Numerical Investigation." *Applied Optics* 41: 3075-83.

[3] Deinega, A., Valuev, I., Potapkin, B., and Lozovik, Y. 2011. "Minimizing Light Reflection from Dielectric Textured Surfaces." *JOSA A* 28: 770-7.

[4] Bouhafs, D., Moussi, A., Chikouche, A., and Ruiz, M. 1998. "Design and Simulation of Antireflection Coating Systems for Optoelectronic Devices Application to Silicon Solar Cells." *Solar Energy Materials and Solar Cell* 52: 79-93.

[5] Sopori, B. L., and Pryor, R. A. 1983. "Design of Antireflection Coatings for Textured Silicon Solar Cells." *Solar Cells* 8: 249-61.

[6] Redfield, D. 1981. "Method for Evaluation of Antireflection Coatings." *Solar Cells* 3 (1): 27-33.

[7] Pedrotti, F. L., Pedrotti, L. S., and Pedrotti, L. M., 2007. *Introduction to Optics.* 3rd ed. Upper Saddle River, NJ: Pearson Prentice Hall.

[8] Oraizi, H., and Afsahi, M. 2009. "Transmission Line Modeling and Numerical Simulasion for the Analysis and Optimum Design of Metamaterial Multilayer Structures." *Progress in Electromagnetics Research B* 14: 263-83.

[9] Chen, H., Zhou, J., Hara, J., Chen, F., Azad, A. K., and Taylor, A. K. 2010. "Antireflection Coating Using Metamaterials and Identification of Its Mechanism." *Phys. Rev. Lett.* 105 (7): 073901.

[10] Pillai, S., Catchpole, K. R., Trupke, T., and Green, M. A. 2007. "Surface Plasmon Enhanced Silicon Solar Cells." *J. Appl. Phys.* 101: 093105.

[11] Hägglund, C., Zäch, M., Petersson, G., and Kasemo, B. 2008. "Electromagnetic Coupling of Light into a Silicon Solar Cell by Nanodisk Plasmons." *Appl. Phys. Lett.* 92: 053110.

[12] Lee, H. C., Wu, S. C., Yang, T. C., and Yen, T. J. 2010. "Efficiently Harvesting Sun Light for Silicon Solar Cells through Advanced Optical Couplers and a Radial p-n Junction Structure." *Energies* 3 : 784-802.

[13] Stuart, H. R., and Hall, D. G. 1998. "Island Size Effects in Nanoparticle-Enhanced Photo Detectors." *Appl. Phys. Lett.* 73: 3815-7.

[14] Schaadt, D. M., Feng, B., and Yu, E. T. 2005. "Enhanced Semiconductor Optical Absorption via Surface Plasmon Excitation in Metal Nanoparticles." *Appl. Phys. Lett.* 86: 063106.

[15] Qu, D., Liu, F., Yu, J., Xie, W., Xu, Q., Li, X., and Huang, Y. 2011. "Plasmonic Core-Shell Gold Nanoparticle Enhanced Optical Absorption in Photovoltaic Devices." *Appl. Phys. Lett.* 98:113119.

[16] Wang, E. C., Mokkapati, S., Soderstrom T., Varlamov, S., and Catchpole, K. R. 2013. "Effect of Nanoparticle Size Distribution on the Performance of Plasmonic Thin-Film Solar Cells: Monodisperse versus Multi-disperse Arrays." *IEEE J. Photovolt* 3: 267-70.

[17] Temple, T. L., Mahanama, G. D. K., Reehal, H. S., and Bagnall, D. M. 2009. "Influence of Localized Surface Plasmon Excitation in Silver Nanoparticles on the Performance of Silicon Solar Cells." *Sol. Energy Mater. Sol. Cells* 93: 1978-85.

[18] Atwater, H. A., and Polman. A. 2010. "Plasmonics for Improved Photovoltaic Devices." *Nature Materials* 9 (3): 205-13.

[19] Ubeid, M. F., and Shabat, M. M. 2016. "Numerical Study of Antireflection Coatings in Waveguide Structures with Silicon Nanoparticles Interlayer." *Journal of Modern Optics* 64: 374-8.

[20] Shabat, M. M., El-Amassi, D. M., Daniel, M., and Schaadt, D. 2016. "Design and Analysis of Multilayer Waveguides with Different Substrate Media and Nanoparticles for solar Cells." *Solar Energy Journal* 137: 409-12.

[21] Chung, K., Kim, R., Chang T., and Shin, J. 2016. "Optical Effective Media with Independent Control of Permittivity and Permeability Based on Conductive Particles." *Applied Phys. Letter* 109: 021114.

[22] Poxson, D. J. et al. 2009. "Broadband Omnidirectional Antireflection Coatings Optimized by Genetic Algorithm." *Opt. Lett.* 34 (6): 728-30.

[23] Hamouche, H., and Shabat, M. M. 2016. "Enhanced Absorption in Silicon Metamaterials Waveguide Structure." *Appl. Phys.* 122 (7): 1-7.

[24] Park, J. S., Rao, J., Kim, T., and Varlamov, S. 2013. "Highest Efficiency Plasmonic Poly-Crystalline Silicon Thin-Film Solar Cells by Optimization of Plasmonic Nanoparticle Fabrication." *Plasmonics* 8:1209.